ISSN: 2277-9655
(I2OR), Publication Impact Factor: 3.785

IJESRT

INTERNATIONAL JOURNAL OF ENGINEERING SCIENCES & RESEARCH TECHNOLOGY

NONLINERA COUPLING ANALYSIS FOR HYPERSONIC FLIGHT VEHICLE

Erlong Su*, Jianjun Luo
Science and Technology on Aerospace Flight Dynamics Laboratory
Northwestern Polytechnical University, Xi'an, China, 710072

ABSTRACT

Based on 3D figuration, the nonlinear coupling between the airframe and scramjet for hypersonic vehicle is investigated in this paper. Firstly, a free-free beam structure elastic model is utilized taking into account of varying cross-section moment of inertia and uneven mass, and 3D elastic deformations are introduced. Then, the coupling dynamic equation is established and the coupling characteristics among the 3D aerodynamics, structure elastic deformation and propulsion are analyzed. The solution of the thrust force and its relation with the elastic deformation are presented and analyzed qualitatively and quantitatively. The results show that the elastic deformation of the structure affects the thrust force of scramjet significantly which provide very important information for the operation of scramjet and control of hypersonic vehicle

KEYWORDS: Hypersonic vehicle; Coupled dynamic modeling; Structural elastic deformation; Scramjet

INTRODUCTION

Because of the highly integrated airframe/propulsion and tight coupling among the structure elastic deformation, aerodynamics and propulsion by nature, hypersonic vehicle dynamic modeling and control strategy are much more complicated and challenging than conventional flight vehicle. In literature[1], the authors described the development of one of the first control-relevant 3-DOF (degree of freedom) models for a generic hypersonic vehicle based on the first principle. Aerodynamic forces were calculated using the classical 2D Newtonian impact theory. The quasi-one-dimensional, quasi-steady flow was applied in the scramjet model. Rigid airframe and 2D scramjet propulsion system were utilized for dynamic modeling and control of hypersonic vehicles in[2-5]. However, due to large structure elastic deformation of the slender and light structure for hypersonic vehicle, the rigid model cannot reflect true dynamic characteristics of hypersonic vehicle. Improved modeling precision was achieved based on 2D aerodynamics and uneven mass free-free beam structure elastic model in [6-9]. The 3D configuration model was applied in literature [10], but the model did not incorporate the coupling between the structure elastic deformation and propulsion. The work in [11] focused on enhancing the fidelity of the hypersonic vehicle control surfaces by considering the unsteady aerodynamics, aerothermal heating, and the resulting material property degradation of the control surface structure through using structural Ritz modes and proper orthogonal decomposition of the dominant thermal modes. A kriging ROM of the Stanton number was created in [12] as part of comparison of reduced models for computational aerothermodynamics. A partitioned-based, multi-physics, multi-fidelity simulation framework for flexible hypersonic vehicles was developed and implemented in [13].

In this paper. Firstly, longitudinal free-free beam structure elastic model taking into account of varying cross-section moment of inertia and uneven mass is constructed and calculated by assumed modes method, the mode shapes for the 3D meshed configuration are given according to the projection relations between the elastic beam and 3D configuration. Secondly, the coupling dynamic equation is presented and the coupling relations among the 3D aerodynamics, structure elastic deformation and propulsion are analyzed. Lastly, thrust force is calculated based on one-dimensional scramjet engine model, the impacts of structure elastic deformation on the propulsion are analyzed qualitatively and quantitatively.

MODELING AND ANALYSIS OF ELASTIC STRUCTURE

One of the generic hypersonic vehicles being utilized here is the waverider-like hypersonic cruising vehicle as shown in Figure 1.

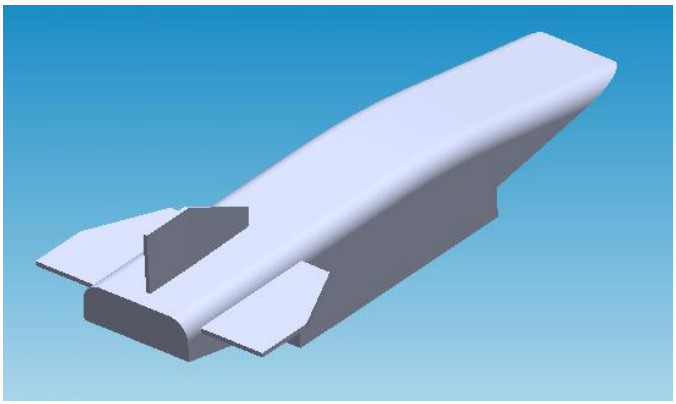

Figure 1. Hypersonic vehicle figuration

The conceptual parameters for the hypersonic vehicle are given in Table 1.

Table 1. The conceptual parameters for the hypersonic vehicle

Name	Symbol	Value
Vehicle length	L	$30m$
Vehicle mass	M	$1.69 \times 10^5 kg$
Wings span	L_1	$3.5m$
Vehicle span	L_2	$13m$
Moment of inertia about x-axis	I_{xx}	$3.19 \times 10^6 kg.m^2$
Moment of inertia about y-axis	I_{yy}	$2.82 \times 10^7 kg.m^2$
Moment of inertia about z-axis	I_{zz}	$2.64 \times 10^7 kg.m^2$
First modal generalized mass	m_1	$523.9413 kg.m^2$
Second modal generalized mass	m_2	$679.4542 kg.m^2$
Third modal generalized mass	m_3	$714.1397 kg.m^2$

Based on structure layout of the hypersonic vehicle, the variation of the cross-section moment of inertia alongside the longitudinal can be obtained. The contrast of varying cross-section moment of inertia with the constant cross-section moment of inertia along the longitudinal is depicted in Figure 2.

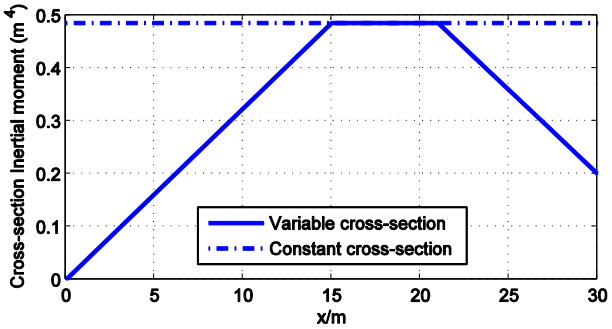

Figure 2. Variation of cross-section moment of inertia along longitudinal

Taking into account of the varying cross-section moment of inertia and uneven mass to the establishment of structure elastic model, The free-free beam structure elastic model are formulated as follows

$$\frac{\partial^2}{\partial x^2}[E(x)I(x)\frac{\partial^2 y(x)}{\partial x^2}] + m(x)\frac{\partial^2 y(x)}{\partial t^2} = 0 \quad (1)$$

The natural frequencies and mode shapes for the varying cross-section moment of inertia and uneven mass free-free

beam structure elastic model are computed using assumed modes method[7]. The assumed modes are utilized by basic functions ω_i for mode shapes of the flight vehicle that corresponds to the analytical solution to the transverse vibration of a free-free beam. The computational efficiency and accuracy of make this approach unparalleled. The first three mode shapes are given in Figure 3. In this paper, the surface of 3D hypersonic vehicle is meshed by triangular surface panels. Each panel is triangular, such that it will remain planar under arbitrary elastic deformation. The Figure 4 shows lateral view of the 3D meshed hypersonic vehicle. It is assumed that each cross-section of the undeformed configuration perpendicular to the undeformed elastic axis still maintain planar and normal to the elastic axis as model deforms.

Figure 5 to Figure 6, the deformations of 3D configuration for different modes and their combination are achieved when their generalized coordinates are 10. It is obvious that the 3D configuration deformation can truly unveil the variation of the aerodynamics and capture coupling relations among the aerodynamics, structure elastic deformation and propulsion in more detail.

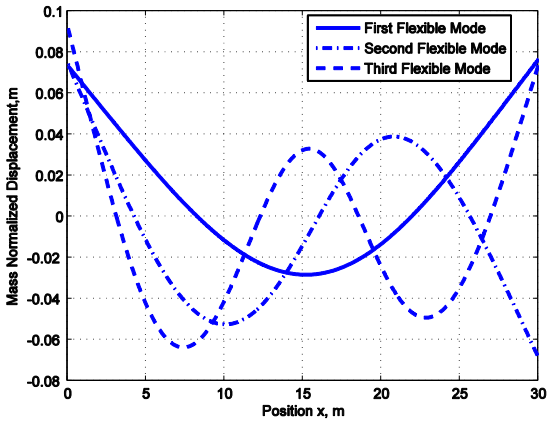

Figure 3. The first three elastic modes of free-free beam

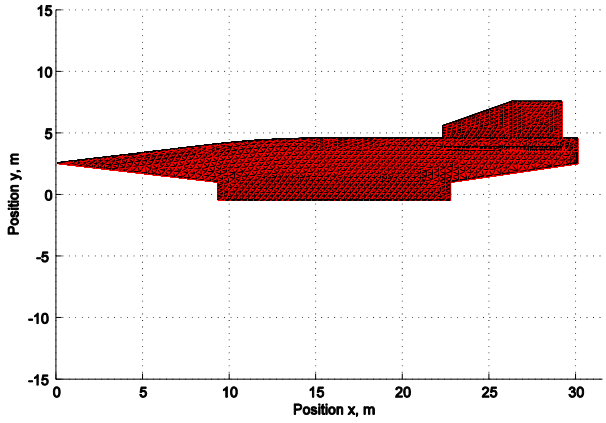

Figure 4. Lateral view of the undeformed hypersonic vehicle

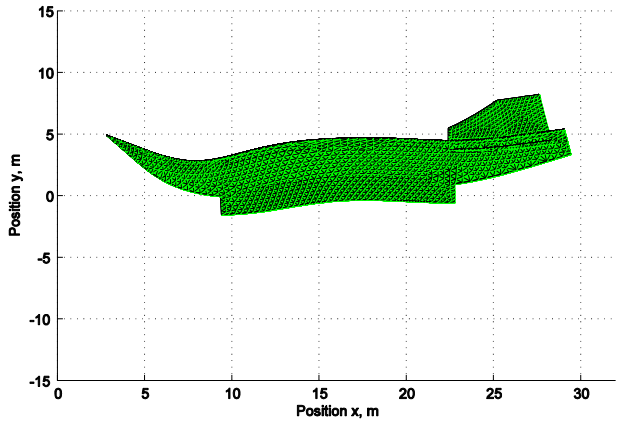

Figure 5. Elastic deformation of combination for the first three modes

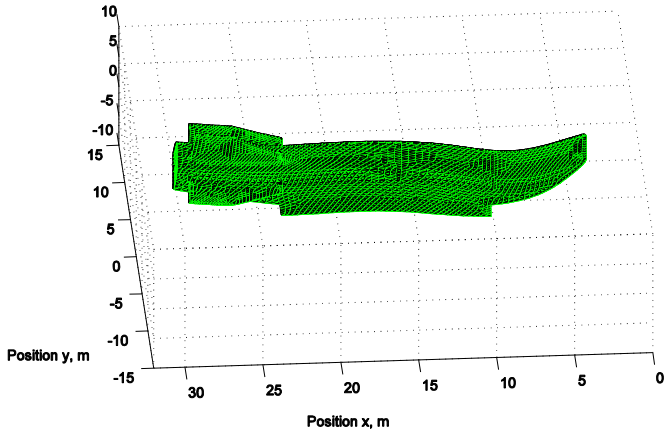

Figure 6. Elastic deformation of combination for the first three modes in 3D view

COUPLED DYNAMIC MODELING

The following section is the establishment of dynamic model as well as the computation of propulsion performance and aerodynamics.

Coupled Dynamic Equations

The longitudinal dynamics of a flexible aircraft is written as[15]

$$\begin{cases} \dot{V} = [\frac{Tcos(\alpha)-D}{m}] - gsin(\gamma) \\ \alpha = -[\frac{L+Tsin(\alpha)}{mV}] + q + [\frac{g}{V} - \frac{V}{R_E+h}]cos(\gamma) \\ \dot{q} = \frac{M}{I_{yy}} \\ \dot{h} = Vsin(\gamma) \\ \dot{\theta} = q \\ \ddot{\eta}_{y,i} = -2\zeta\omega_i\dot{\eta}_{y,i} - \omega_i^2\eta_{y,i} + \frac{N_{y,i}}{m_i} \quad i = 1,2,3 \\ \gamma = \theta - \alpha \\ g = g_0[\frac{R_E}{R_E+h}]^2 \end{cases} \tag{2}$$

$$\begin{cases} X = \frac{Tcos(\alpha)-D}{m} \\ Z = -\frac{Tsin(\alpha)+L}{m} \\ F = \frac{M}{I_{yy}} \end{cases} \tag{3}$$

where h denotes the altitude, V denotes the velocity, α denotes the attack angle, θ and q denote the pitch angle and the pitch angle rate. These five states are rigid states; $\eta_{y,1}, \dot{\eta}_{y,1}, \eta_{y,2}, \dot{\eta}_{y,2}, \eta_{y,3}, \dot{\eta}_{y,3}$ denote the first elastic mode

generalized coordinate, first elastic mode generalized coordinate rate, second elastic mode generalized coordinate and the second elastic mode generalized coordinate rate as well as third elastic mode generalized coordinate and the third elastic mode generalized coordinate rate, respectively. These six states are elastic states. The control inputs consist of elevator deflection angle δ_e and fuel equivalence ratio ϕ, which can change the lift L, drag D, pitch moment M, thrust force $T$and generalized force N_i directly and indirectly. Where generalized mass of the i mode is defined as[14][15]

$$m_i = \int_V \phi_i \phi_i \rho dV \tag{4}$$

The first, second and third generalized forces are being expressed as

$$\begin{cases} N_{y,1}(t) = \int_x \int_z \phi_1(x) p(x,t) dz dx + \sum_{j=1}^{l} \phi_1(x_j) p_j(t) \\ N_{y,2}(t) = \int_x \int_z \phi_2(x) p(x,t) dz dx + \sum_{j=1}^{l} \phi_2(x_j) p_j(t) \\ N_{y,3}(t) = \int_x \int_z \phi_3(x) p(x,t) dz dx + \sum_{j=1}^{l} \phi_3(x_j) p_j(t) \end{cases} \tag{5}$$

where $N_{y,1}(t), N_{y,2}(t), N_{y,3}(t)$ denote the first, second and third generalized forces, ϕ_1, ϕ_2, ϕ_2 denote the first, second and third mode shapes. $p(x,t)$ is the longitudinal aerodynamic pressure component which acts on the exterior panels of the hypersonic vehicle. The pressure is a function of the attack angle, velocity and so on, more specifically, $p(\alpha, V, h, \eta_{y,1}, \eta_{y,2}, \eta_{y,3} \cdots)$; $p_j(t)$ is the concentrated force acting on the elevator; l is the number of the concentrated force.

The equations above reflect the relations among the structure elastic deformation, aerodynamics and propulsion. Through the change of generalized coordinates $\eta_{y,1}, \eta_{y,2}, \eta_{y,3}$, the elastic deformation affect the lift L, drag D, pitching moment M and thrust force T. There are three coupling sub-loops among the coupling of aerodynamics, structure elastic deformation and propulsion.

1). The coupling between the aerodynamics and structure elastic deformation

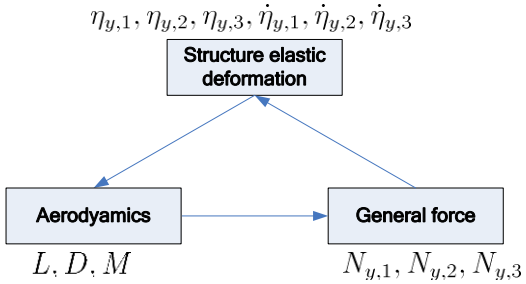

Figure 7. Coupling relationship of structure elastic deformation and aerodynamics

The coupling relation concerning about structure elastic deformation and aerodynamics is presented in Figure 7. The variation of generalized coordinates $\eta_{y,1}, \eta_{y,2}, \eta_{y,3}$ will change the steady aerodynamics of the hypersonic vehicle. The corresponding changing rate of generalized coordinates $\dot{\eta}_{y,1}, \dot{\eta}_{y,2}, \dot{\eta}_{y,3}$ will induce the unsteady aerodynamics and then alter the pressure distribution over the flight vehicle, the generalized forces, to be specific, the $N_{y,1}(t), N_{y,2}(t), N_{y,3}(t)$ chiefly dependent on surface pressure will be changed accordingly; And eventually the varying generalized forces will change the corresponding generalized coordinates and generalized coordinates rate individually.

2). The coupling between the propulsion and structure elastic deformation

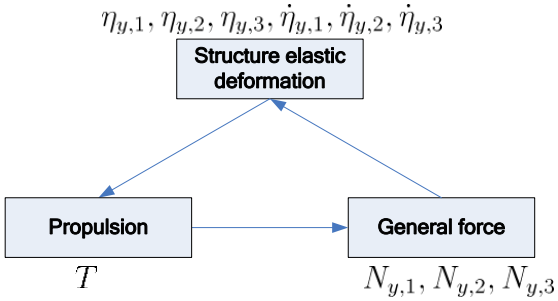

Figure 8. Coupling relationship of structure elastic deformation and propulsion

The coupling relation given above is the interplay of structure elastic deformation and propulsion as shown in Figure

8. The change of generalized coordinates $\eta_{y,1}, \eta_{y,2}, \eta_{y,3}$ will alter the scramjet inlet shape and exit external nozzle shape which will change the inlet condition (Mach number and mass flow rate)and external nozzle condition (pressure along the external nozzle, due to the highly sensitive of scramjet to the inlet condition, finally it will significantly influence the thrust of scramjet performance. While the variation of the thrust force and afterbody (external nozzle) force will affect the generalized forces similarly, which results in the change of generalized coordinates and their changing rate, simultaneously.

3). The coupling between the propulsion and aerodynamics

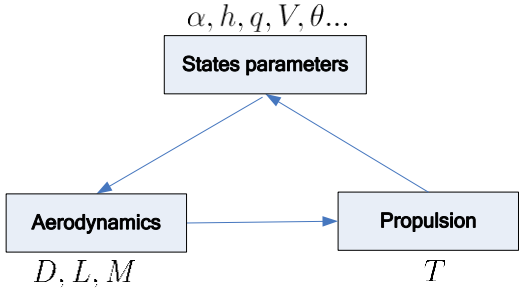

Figure 9. Coupling relationship of aerodynamics and propulsion

The interaction of aerodynamics and propulsion is presented in Figure 9. Because of the highly integrated airframe and propulsion, the forebody and afterbody of the airframe which mainly contribute to the aerodynamics are inherently the inlet and external nozzle of the scramjet, so there exists a strong coupling between the aerodynamics and thrust force. The change of the state parameters, such as α, h, q, V, will dramatically affect the aerodynamics and thrust, vice versa.

The overall coupling relations of structure elastic deformation, aerodynamics and propulsion are represented in Figure 10.

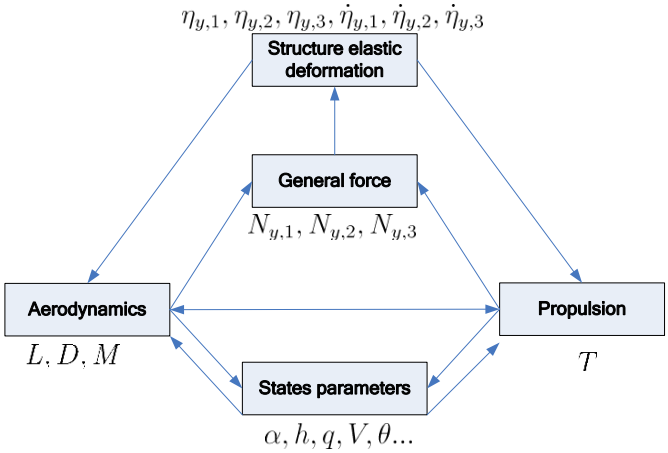

Figure 10. Coupling relations among structure elastic deformation, aerodynamics and propulsion

Modeling of Propulsion and Thrust Calculation

From the view of dynamic model, the scramjet can be divided into three parts consisting of the diffuser, combustor and inner nozzle as shown in Figure 11[6]

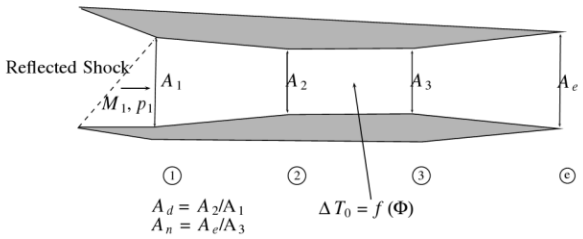

Figure 11. Geometry of scramjet

where A_1, A_2, A_3, A_e denote the diffuser inlet area, combustor inlet area, inner nozzle inlet area and the exterior nozzle area. The thrust force is calculated using the formula as below [6]

$$T = \dot{m}_\alpha(V_e - V_\infty) + (p_e - p_\infty)A_e - (p_1 - p_\infty)A_1 \quad (6)$$

where $\dot{m}_\alpha$ denotes the mass flow rate of the air; V_∞, p_∞denote the free stream velocity and pressure; V_e, p_e denote the exit velocity and pressure.

The pressure at any point on the afterbody is given by Chavez and Schmidt [9] as follows

$$\mathrm{p}_\alpha = \frac{p_e}{1+x_\alpha/L_\alpha(p_e/p_\infty-1)} \quad (7)$$

The x and z body axis forces due to the afterbody pressure are written as

$$F_{x,\alpha} = p_\infty L_\alpha \frac{p_e}{p_\infty}\frac{ln\frac{p_e}{p_\infty}}{\frac{p_e}{p_\infty}-1}tan(\lambda) \quad (8)$$

$$F_{z,\alpha} = -p_\infty L_\alpha \frac{p_e}{p_\infty}\frac{ln\frac{p_e}{p_\infty}}{\frac{p_e}{p_\infty}-1} \quad (9)$$

where L_α, λ denote the external nozzle length and angle.

Relation of the thrust force, the equivalence ratio and the attack angle is presented in Figure 12, and relations of the propulsion moment, the equivalence ratio and the attack angle is presented in Figure 13. It is indicated in the two figures that the increase of the attack angle and the equivalence ratio will lead to the augment of the thrust force and the thrust moment.

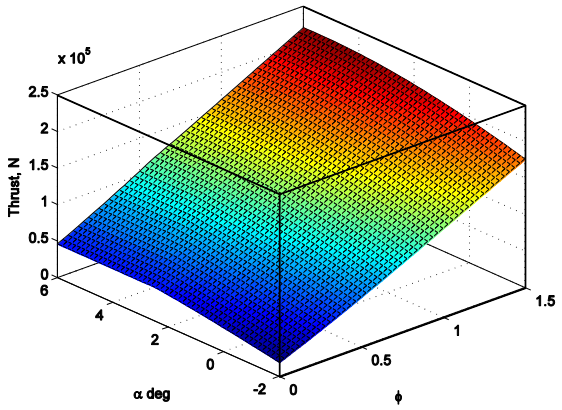

Figure 12. Relationship among thrust force, ϕ and attack angle

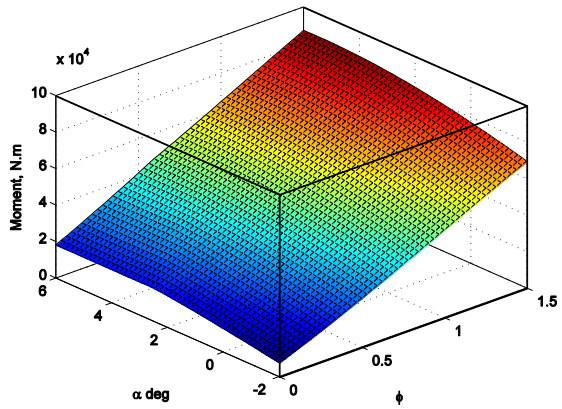

Figure 13. Relationship among thrust moment, ϕ and attack angle

There exists a strong nonlinear coupling between the elastic deformation and scramjet. Here, the double oblique

ISSN: 2277-9655
(I2OR), Publication Impact Factor: 3.785

shocks are used to replace the single shock oblique to approximate the shock change induced by elastic deformation of the forebody and the afterbody. The nonlinear influence of elastic deformation of the forebody and the afterbody to the thrust of scramjet are shown in the following figures.

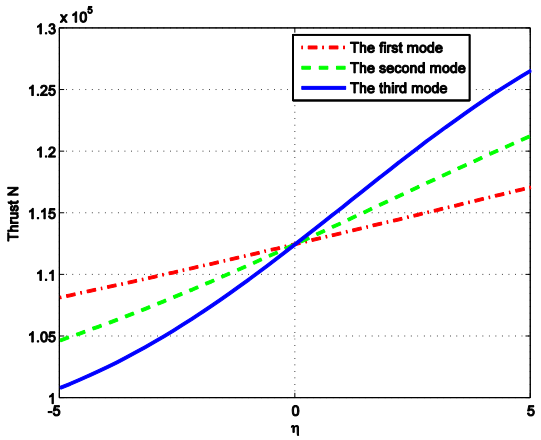

Figure 14. Forebody induced thrust changing due to the structure deformation

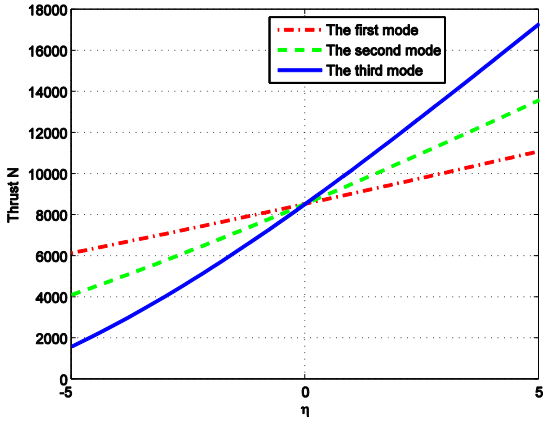

Figure 15. Afterbody induced thrust changing due to the structure deformation

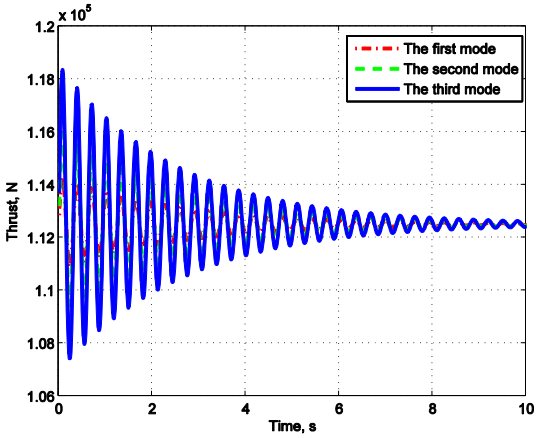

Figure 16. Forebody induced thrust vibration due to the structure vibrating deformation

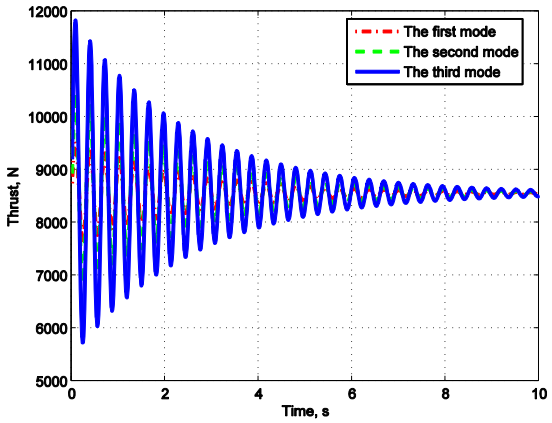

Figure 17. Afterbody induced thrust vibration due to the structure vibrating deformation

Figure 14 plots the forebody induced thrust changing due to the structure deformation for different elastic modes with generalized coordinates varying from -5 to 5. While Figure 15 gives the afterbody induced thrust changing due to the structure vibration for different elastic modes. Figure 16 and Figure 17 plot the forebody induced thrust vibration and afterbody induced thrust vibration due to the structure vibration for different elastic modes. As for aforebody, the induced thrust change due to the structure vibrating deformation is around 6% of the averaged value maximally. While as for afterbody induced thrust change, we can see that thrust change due to the structure vibrating deformation by afterbody is around 30% of the averaged value maximally. The results show that the elastic deformation of the structure affects the thrust force of scramjet significantly.

CONCLUSION

The pursuing of high fidelity dynamic model is still the focus for the control system design and is of the great concern for the conceptual design of hypersonic vehicle. In this paper, through analyzing the coupling among the aerodynamics, structure elastic deformation and propulsion, the coupled dynamic model taking into account of 3D aerodynamics and varying cross-section inertia and uneven mass free-free beam model as well as panel friction force is established. Then the one-dimensional scramjet model is applied to calculate the thrust force, the relations between structure elastic deformation and propulsion are analyzed qualitatively and quantitatively. The results show that the elastic deformation of the structure affects the thrust force of scramjet significantly .In the future work, the application of the robust control method to the hypersonic vehicle will be further studied.

REFERENCES

[1] Chavez, F., and Schmidt, D., "Analytical Aeropropulsive/Aeroelastic Hypersonic-Vehicle Model with Dynamic Analysis," Journal of Guidance, Control, and Dynamics, Vol. 17, No. 6, 1994, pp. 1308-1319.
[2] Obaid Ur Rehman, Barı¸s Fidan, "Uncertainty Modeling for Robust Multivariable Control Synthesis of Hypersonic Flight Vehicles," AIAA 2009-7288, 2009.
[3] Lael von Eggers Rudd1, John Hodgkinson, "Hypersonic Stability Derivative Modeling Issues," AIAA 2010-7929, 2010.
[4] Derek J. Dalle, Michael A. Bolender, "Flight Envelope Calculation of a Hypersonic Vehicle Using a First Principles-Derived Model," AIAA 2011-2368, 2011.
[5] Sanketh Bhat, Felipe A. C. Viana. "Control-Oriented Design using H-inf Synthesis and Multiple Surrogates," AIAA 2010-3089, 2010.
[6] M.A.Bolenderand, D. B. Doman, "Nonlinear Longitudinal Dynamical Model of an Air-Breathing Hypersonic Vehicle," Journal of Spacecraft and Rockets, Vol. 44, No. 2, 2007, pp. 374-387.
[7] Williams T., Bolender, M. A., and Doman, D. B, "An Aerothermal Flexible Mode Analysis of a Hypersonic Vehicle," AIAA 2006-6647, 2006.

[8] Jason. T. Parker., Andrea. Serrani., "Control-Oriented Modeling of an Air-Breathing Hypersonic Vehicle," Journal of Guidance, Control, and Dynamics, Vol. 30, No. 3, 2007, pp.856-869.
[9] Sanketh. Bhat., Rick. Lind., "Control-oriented Design of Operating Range for Linear Parameter Varying Systems for Closed-Loop Performance," AIAA 2010-8412, 2010.
[10] Scott G. V. Frendreis., and Carlos E. S. Cesnik., "3D Simulation of Flexible Hypersonic Vehicles," AIAA 2010-8229, 2010.
[11] Falkiewicz, N.J. and Cesnik, C.E.S., "Proper Orthogonal Decomposition of Reduced-Order Thermal Solution in Hypersonic Aerothermoelastic Simulations," AIAA Journal, Vol. 49, No. 5, 2011, pp. 994-1009.
[12] Crowell, A.R. and McNamara, J.J., "Model Reduction of Computational Aerothermodynamics for Hypersonic Aerothermoelasticity," AIAA Journal, Vol. 50, No. 1, 2012, pp. 74-84.
[13] Ryan J. Klock and Carlos E.S. Cesnik, "Aerothermoelastic Simulation of Air-Breathing Hypersonic Vehicles," AIAA 2014-0149, 2014.
[14] Meirovitch, L., Analytical Methods in Vibrations, MacMillan, New York,1967, pp. 135-143 ,161-163.
[15] Martin R. Waszak., David K. Schmidt., "Flight Dynamics of Aeroelastic Vehicles," Journal of aircraft. Vol. 25, No. 6, 1988, pp.563-571.